RESCIENCE C

Replication / ML Reproducibility Challenge 2020

[Re] A Reproduction of Ensemble Distribution Distillation

Toomas Liiv[1,2], Einar Lennelöv[1,2], and Aron Norén[1,2]
[1]Equal contribution – [2]KTH Royal Institute of Technology, Stockholm, Sweden

Edited by
Koustuv Sinha

Reviewed by
Anonymous Reviewers
A Reproduction of Ensemble Distribution Distillation

Received
15 February 2020

Published
21 May 2020

DOI
10.5281/zenodo.3818623

Reproducibility Summary

Scope of Reproducibility

The authors claim that their proposed method is able to, given an ensemble of deep neural networks, capture the uncertainty estimation and decomposition capabilities of the ensemble into a single model. The authors also claim that this only results in a small reduction in classification performance compared to the ensemble. We examine these claims by reproducing most of the authors' experiments on the CIFAR-10 dataset.

Methodology

The proposed method was re-implemented in `tf.keras`. The surrounding data pipelines, pre-processing, and experimentation code were also re-implemented. As in the original paper, the models were based on VGG-16 networks trained from scratch with random initialization. Training and evaluation was done on two consumer-grade GPUs, for a total of 273 hours.

Results

Our findings support the authors' central claims. In terms of uncertainty estimation our EnD^2 achieved (99 ± 1) % of the AUC-ROC of our ensemble on the OOD-detection task. The corresponding value in the original paper was (100 ± 1) %. In terms of classification our EnD^2 had (16 ± 1)% higher error than our ensemble. The corresponding values in the original paper was (11 ± 6)%. Other metrics showed similar agreement, but, significantly, in the OOD-detection task our EnD performed at least as well as our EnD^2. This is in stark contrast with the original paper.
We also took a novel approach to visualizing the uncertainty decomposition by plotting the resulting distributions on a simplex, offering a visual explanation to some surprising results in the original paper, while mostly supporting the authors' intuitive justifications for the model.

What was easy

The original paper features a thorough mathematical formulation of the method, aiding conceptual understanding. The datasets used by the authors are publicly available. The

Correspondence should be addressed to Toomas Liiv (toomasl@kth.se)
The authors have declared that no competing interests exist.
Code is available at https://github.com/lennelov/endd-reproduce. – SWH swh:1:dir:2c366708175b2ed7c83ce6b33a80dd43c8aad915.
Open peer review is available at https://openreview.net/forum?id=p1BXNUcTFsN.

use of the simpler datasets also meant that it was computationally feasible for us to reproduce these results. The base model used is well known with several implementation available, allowing us to focus on the novel aspects of the method.

What was difficult

While the theoretical explanations of the method are excellent, we initially found it hard to translate this into an implementation. Our difficulty was likely caused by our inexperience with the subject matter. Nonetheless, a pseudocode, such as the one we have provided, would havee simplified the re-implementation. We were not able to reproduce the results on some of the datasets due to limited computational resources.

Communication with original authors

We did not contact the original authors directly, but we did refer to a public GitHub and blog post created by one of the authors. At the same time as submitting this report to the ML Reproducibility Challenge 2020 we also sent a copy to the authors and asked for their feedback.

1 Introduction

Uncertainty estimation can help to make deep learning safer and more usable by allowing the model to identify cases it is not suitable to handle. There are different kinds of uncertainty, however, and it is especially interesting to separate uncertainty caused by ambiguities or contradictions in the data from the uncertainty that arises when a model faces a situation it has not been trained for. Ensemble-based methods of uncertainty estimation are capable of making this distinction but suffer from computational requirements at the evaluation phase [1]. The authors of *Ensemble Distribution Distillation* (EnD^2) [2] address this issue by using the output of an ensemble to train a so-called Prior Network (PN) [3], distilling the ensemble down to a single model while also preserving its uncertainty decomposition abilities. This can be contrasted with regular ensemble distillation models [4] (EnD), which are not able to decompose uncertainty. The reproduced paper was accepted to ICLR2020.

2 Scope of reproducibility

We consider the setting of using CIFAR10 [5] as an in-distribution dataset, and LSUN [6] as an out-of-distribution dataset. Our supplementary material also examines the setting of using a synthetic dataset in $\mathbb{R}^2$ for visualization.
The claims from the original article that this reproduction is testing are as follows:

1. **Classification performance**: In terms of error rate, prediction rejection rate, and negative log-likelihood EnD^{2}has worse performance than the ensemble, but similar performance to EnD and PriorNet, and better performance than the individual model. In terms of expected calibration error, EnD^2 has worse performance than the ensemble, but better performance than the other methods. On CIFAR-10 in particular, EnD^2 has the best expected calibration error of all models. This claim corresponds to Table 3 in the original paper.

2. **Out-of-distribution detection performance**: In terms of AUC-ROC on CIFAR-10 vs. LSUN, EnD^2 without auxiliary dataset performs worse than the ensemble and the PriorNet, similar to the individual model, and better than EnD. With the auxiliary dataset, however, EnD^2 performs as well as the ensemble, almost as well as PriorNet, and better than EnD. Using knowledge uncertainty as opposed to total uncertainty on CIFAR-10 vs. LSUN does not yield an improved AUC-ROC. This claim corresponds to Table 4 in the original paper.

3. **Dependency on ensemble size**: Using 20 models in the ensemble does better than using 5 models, but there is no conclusive gain when using more than 20 models.

4. **Dependency on temperature**: It is necessary to use temperature of at least 5 to successfully distribution-distill the ensemble. Using higher initial temperatures do not result in conclusive improvement.

5. **Uncertainty decomposition**: EnD^2 trained with an auxiliary dataset is able to reconstruct the uncertainty decomposition made possible by ensembles.

We reproduce all experiments of the main article and most of the appendix, except for the use of CIFAR100 and Tiny Imagenet datasets. Some of these results can be found in our supplementary material. From their appendix, we do not reproduce Table 7 in appendix B. We did not recreate the OOD-detection plots when reproducing the ablation study.

Table 1. Datasets used in the CIFAR-10 setting

Dataset	Samples	Classes	Dimensions	Link
CIFAR-10 train	50000	10	32x32x3	https://www.cs.toronto.edu/ kriz/cifar.html
CIFAR-100 train	50000	100	32x32x3	https://www.cs.toronto.edu/ kriz/cifar.html
CIFAR-10 test	10000	10	32x32x3	https://www.cs.toronto.edu/ kriz/cifar.html
LSUN test	10000	10	256x256x3	https://www.yf.io/p/lsun

3 Methodology

3.1 Model description

We consider the same seven models as the original authors:

- IND: A single classification model.
- ENSM: An ensemble of independently trained IND models.
- EnD: A single model distilling ENSM trained according to [4].
- EnD^2: A single model distribution-distilling ENSM trained according to [2].
- EnD$_{+\text{AUX}}$: Like EnD, but trained with auxiliary data.
- EnD$^2_{+\text{AUX}}$: Like EnD^2, but trained with auxiliary data.
- PN$_{+\text{AUX}}$: A PriorNet model with auxiliary data trained according to [3]

These models are all based on almost identical VGG16 architectures [7], adapted to CIFAR-10 data as in [3] by adding dropout, batch normalization and reducing the size of the fully connected layers. The only exception being that batch normalization is not used for PN.

3.2 Dataset

The training set of CIFAR-10 was used as the primary training dataset. The training set of CIFAR-100 was used as an auxiliary dataset. For evaluating the classification task the test set of CIFAR-10 was used. For evaluating the out-of-distribution detection task the CIFAR-10 test set was used as in-domain dataset, while the LSUN test set was used as the out-of-domain dataset. Information about the datasets is listed in Table 1.
Each image x was normalized according to $x' = x/127.5 - 1$ where the operations are elementwise, causing all values to lie in the range (-1, 1). The LSUN images were also scaled down to 32x32. Furthermore, dataset augmentation was used for all models, consisting of rotations with 15° range, horizontal flips, width and height shifts of up to 4 pixels in each direction, and using nearest-neighbour interpolation.

3.3 Hyperparameters

The models were trained with the hyperparameters listed in Table 2.

3.4 Experimental setup and code

Using these models and dataset we ran a number of experiments, as detailed below. The full code is available on https://anonymous.4open.science/r/4ee2c9ef-295f-44e2-8214-f0818b932817/. Our implementation was made in TensorFlow Keras, as opposed to the original implementation which was made in PyTorch.
Classification: The classification task was evaluated on the test set of CIFAR-10. We use the same four metrics as in the original paper, ERR, PRR, ECE, and NLL. ERR is the mean

Table 2. Training parameters in the CIFAR-10 setting

Model	Epochs	Cycle	η_0	η_{max}	η_{min}	Dropout	T_0	Anneal	AUX data
DNN	45	30	10^{-3}	10^{-2}	10^{-6}	0.5	-	-	-
EnD	90	60	10^{-3}	10^{-2}	10^{-6}	0.7	2.5	No	-
$\text{EnD}_{\text{+AUX}}$	90	60	10^{-3}	10^{-2}	10^{-6}	0.7	2.5	No	CIFAR-100
EnD^2	90	60	10^{-3}	10^{-2}	10^{-6}	0.7	10	Yes	-
$\text{EnD}^2_{\text{+AUX}}$	90	60	10^{-3}	10^{-2}	10^{-6}	0.7	10	Yes	CIFAR-100
PN	45	30	$0.5 \cdot 10^{-3}$	$0.5 \cdot 10^{-2}$	$0.5 \cdot 10^{-6}$	0.7	-	No	CIFAR-100

classification error. PRR is the prediction rejection area ratio introduced in Appendix B of [2]. ECE is the expected calibration error[1]. Finally, NLL is the negative log-likelihood. This experiment tests Claim 1.

Out-of-distribution detection: The OOD-detection task was evaluated with the CIFAR-10 test set as the in-domain set, and the LSUN test set as the out-of-domain set. The AUC-ROC was computed both when total uncertainty and when only knowledge uncertainty is used to make rejection decisions. This experiment tests Claim 2.

Ensemble size ablation study: Our examination of the effect of ensemble size goes slightly beyond the original authors. We extend the error analysis to also consider the sensitivity of EnD^2 to variations in the underlying ensemble. We began by training a set of 400 VGG16 models on CIFAR-10. Next, we sampled randomly from this set to create 4 different sets, each consisting of 100 models.

For each $N \in \{1, 2, 3, 4, 6, 8, 10, 13, 16, 20, 25, 30, 45, 60, 75, 100\}$ we trained four EnD^2 models on an ensemble consisting of the first N models in the first of the four sets, corresponding to what was done in the original study. We also trained *one* model on an ensemble consisting of the first N models *for each* of the three remaining sets, capturing the sensitivity of EnD^2 to changes in the underlying ensemble. All ensemble and EnD^2 models were then evaluated on the classification task. This experiment tests Claim 3.

Temperature ablation study: We reproduce the temperature ablation study by training EnD^2 models for various initial temperatures. For each $T \in \{1, 2, 3, 4, 5, 7.5, 10, 15, 20\}$ we trained three EnD^2 models with initial temperature T on an ensemble consisting of 100 VGG16 models. The EnD^2 models were then evaluated on the classification task. In this experiment, we have chosen to use a slightly finer spacing between the temperatures than what the original authors used. This experiment tests Claim 4.

Simplex visualization: A key motivation for EnD^2 is the idea that an ensemble can distinguish between knowledge uncertainty and data uncertainty, and that this distinction is retained by the EnD^2 model. This is communicated using a schematic figure showing ensemble predictions on a simplex. A similar schematic figure can be found in [3], depicting a Dirichlet PDF of a PriorNet on a simplex. We recreated these figures using experimental data in order to examine Claim 5 from a novel perspective. A new training set was created, consisting of all images from the CIFAR10 train set with one of three labels chosen for their similarity: 'deer', 'horse', and 'dog'. The remaining images were reserved as out-of-distribution dataset for testing. CIFAR-100 was used as auxiliary data. An ensemble and EnD^2 was then trained on this data using the same architecture and processed as before. We then selected various images from the test set and visualized the ensemble predictions as well as the PDF of the EnD^2 model. The simplex visualization was created using open source code [2].

[1] We used the open-source implementation in https://github.com/google/uncertainty-metrics.

[2] http://blog.bogatron.net/blog/2014/02/02/visualizing-dirichlet-distributions/

Table 3. Classification metrics on CIFAR-10. Error bounds signify two standard deviations, taken over three models. Up-arrow (↑) indicates that higher is better, down-arrow (↓) indicates that lower is better.

Crit.	IND	ENSM	EnD	EnD^2	$\text{EnD}_{\text{+AUX}}$	$\text{EnD}^2_{\text{+AUX}}$	$\text{PN}_{\text{+AUX}}$
ERR↓	9.87±0.70	8.80±NA	**8.70**±0.53	9.90±0.20	9.90±0.20	10.17±0.12	10.00±0.35
PRR↑	69.80±1.31	**80.30**±NA	78.67±0.12	76.97±0.83	78.37±1.21	77.20±0.72	56.57±9.49
ECE↓	68.18±0.57	1.65±NA	**1.56**±0.09	2.39±0.22	1.77±0.31	3.04±0.49	9.37±0.62
NLL↓	1.58±0.01	**0.25**±NA	0.26±0.01	0.33±0.00	0.29±0.00	0.34±0.00	0.46±0.00

Table 4. OOD AUC-ROC↑ on CIFAR-10 (in) and LSUN (out). Error bounds signify two standard deviations, taken over three models. Up-arrow (↑) indicates that higher is better, down-arrow (↓) indicates that lower is better.

Unc.	IND	ENSM	EnD	EnD^2	$\text{EnD}_{\text{+AUX}}$	$\text{EnD}^2_{\text{+AUX}}$	$\text{PN}_{\text{+AUX}}$
Tot.↑	86.63±0.31	90.00±NA	89.87±0.46	88.33±0.42	90.60±0.20	90.23±0.12	**92.03**±0.46
Know.↑	-	89.30±NA	-	84.70±1.25	-	88.07±0.46	**90.97**±0.42

3.5 Computational requirements

Training and evaluation were performed on two mid-range consumer GPUs (RTX 2070, GTX 1660s) locally. Regarding VRAM, at least 4711 MiB is required for the models. The total number of GPU time required for the final results is 11.4 GPU days on an RTX 2070. The accumulated GPU days during the reproduction is 3-5 times this amount. We provide detailed numbers in the supplementary materials.

4 Results

4.1 Classification performance

The classification results are shown in Table 3. Overall, the ensemble seems to perform best, and when it does not, it is still within error bounds. Curiously, $\text{EnD}^2_{\text{+AUX}}$ seems to perform worse than the individual model in regards to ERR.

4.2 Out-of-distribution detection performance

The OOD-detection results are shown in Table 4. The results suggest plain EnD^2 performs worse than ENSM, but that the addition of an auxiliary dataset brings the performance up to at least the level of ENSM. More surprising, perhaps, is that EnD^2 seems to perform worse than EnD. In both metrics $\text{PN}_{\text{+AUX}}$ has a significant lead. Using knowledge uncertainty instead of total uncertainty decreases the effectiveness of all tested models. The supplemental material contains histograms showing the distribution of estimated total and knowledge uncertainty over the images.

4.3 Ensemble size ablation study

Figure 1 shows the results of the ensemble size ablation study. The lines 'ENSM Paper' and 'EnD^2 Paper' show the results of the original paper. The bands indicate two standard deviations. Two bands surround the '$\text{EnD}^2_{\text{+AUX}}$' line, representing the two types of variation we have examined. The purple band represents the variation of four EnD^2 models each trained on a different ensemble. The orange band represents the variation of four EnD^2 models all trained on the same ensemble. The band surrounding the '$\text{EnD}^2_{\text{+AUX}}$ Paper' line corresponds to the latter type of variation.

There appears to be a trend of small improvement when the number of models is increased, but the high level of uncertainty makes it difficult to draw conclusions from the remaining points. Nonetheless, the results seem to generally indicate that EnD^2 is not particularly sensitive to ensemble size.

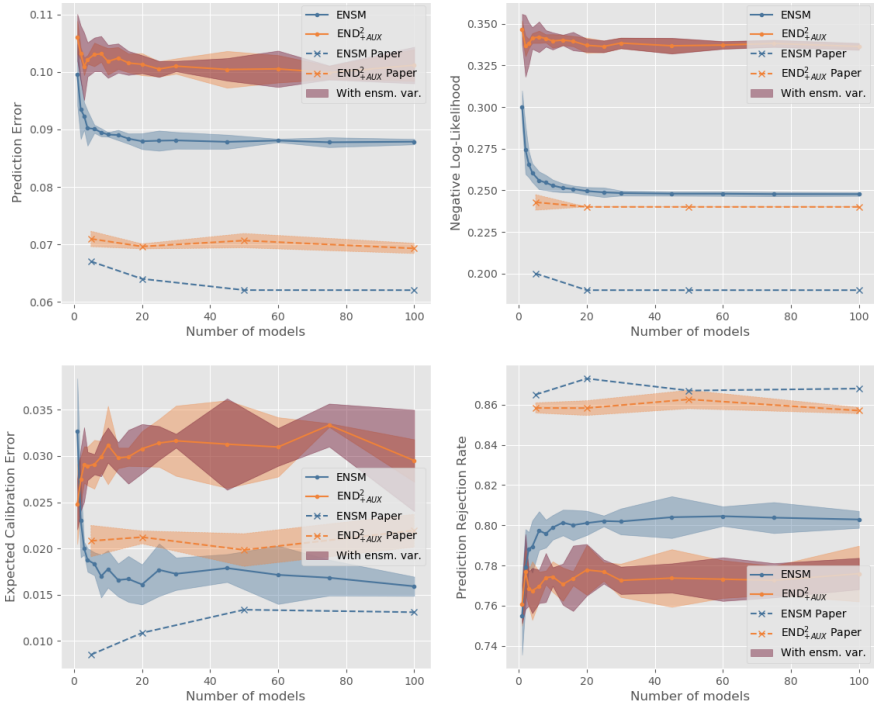

Figure 1. Ensemble size ablation study on CIFAR-10 classification.

4.4 Temperature ablation study

The results of our temperature ablation study are shown in Figure 2, along with the results of the original paper. For initial temperature equal to 1 and 2 our models fail to converge, resulting in poor classification performance. Raising the initial temperature to 3 allows the model to converge. Increasing the initial temperature further has no significant effect.

It is worth noting the negative PRR values for $T = 2$. The original authors mention this possibility when they propose the metric, and offer the interpretation that this means that the model is *increasing* the classification error by rejecting samples, performing worse than simply rejecting at random.

4.5 Simplex visualization

Predictions for four images are visualized in Figure 3. These four images were selected from the CIFAR10 dataset for respectively having the lowest total uncertainty, highest data uncertainty, highest knowledge uncertainty, and highest total uncertainty, as measured by the ensemble. The third row shows the Dirichlet PDF of EnD^2. There is a strong tendency towards extremely sharp distributions, even when the ensemble has high spread, making comparison difficult. For this reason the fourth row plots the PDF after being transformed by the transformation $log(x + 1)$. It is now possible to see that the PDF is adapting to the distribution of the ensembles.

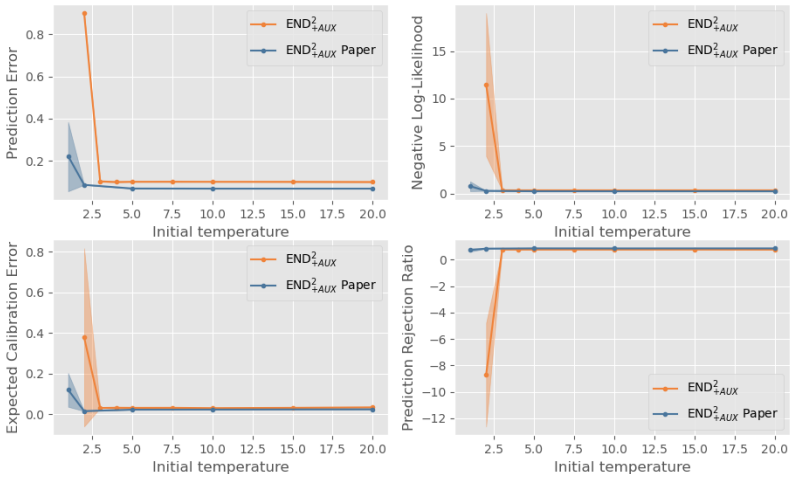

Figure 2. Temperature ablation study on CIFAR-10 classification.

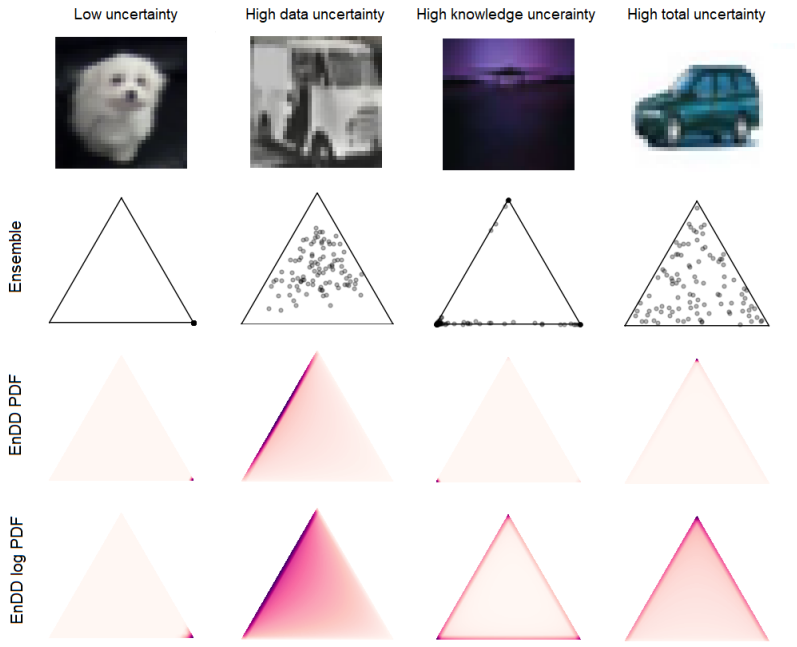

Figure 3. Visualization of ensemble distribution and EnD^2 PDF. The classes are, from left, to top, to right, Deer, Horse and Dog.

Figure 4. Random images from in-domain.

Figure 5. Random images from out-of-domain.

We also plot randomly selected images from the in, out, and auxiliary datasets respectively. The PDF has again been transformed using $log(x + 1)$. Figure 4 shows images from the in-domain dataset, and Figure 5 shows images from the out-of-domain dataset. The PDF appears to follow the ensemble fairly well, but it is noteworthy that the ensembles show such a low degree of spread despite encountering samples on which they have not been trained.

5 Discussion

5.1 Comparison with original paper

We now revisit the six claims which we specified in Section 2.

1. **Classification performance:** When compared to the original table we see overall worse performance. This is likely rooted in the fact that we were unable to achieve as high accuracy on our base VGG16 as in the original article. We therefore instead consider the relative performance between the models. Our supplementary material contains a table allowing for easy comparison with the original results. For example, we find that our EnD^2 has 112.5% of the classification error of the ensemble, while in the original paper this figure is 117.7%. The absolute difference is the same in both papers, 1.1 percentage units. Our results generally agree well, with those of the authors. There are some discrepancies in expected calibration error, but our extremely high ECE for the individual model suggests that there might be an issue in our computations of this metric. Overall our findings support Claim 1.

2. **Out-of-distribution detection performance**: For the most part, our results agree with Claim 2. For instance, we found that using total uncertainty EnD^2 without auxiliary data had 98.1% of the AUC-ROC of the ensemble, while the corresponding figure with auxiliary data was 100.0%. In the original paper, these figures were 96.8% and 99.8% respectively. There is one very significant discrepancy, however. With auxiliary dataset, our EnD^{2}had 99.6% of the AUC-ROC of our EnD, while in the original paper this figure is 106.5%. A similar relationship exists without the auxiliary dataset. It is worth noting that in the original paper EnD performs worse than even the individual model, and the authors themselves note that this is odd. Since EnD^2 is designed to overcome certain shortcomings of EnD in terms of uncertainty estimation we believe that this warrants further investigation.

3. **Dependency on ensemble size**: For prediction error and negative log-likelihood, our results confirm the relative performance between ensembles and EnD$^2_{+\text{AUX}}$, with increased resolution. For expected calibration error, the relative performance is confirmed for a large number of models, but for a small number of models, we get contradictory results. Their results seem to suggest that smaller ensembles have worse calibration, which is not expected, as per [1]. Our results confirm this expectation. In their paper, they state this expectation, but we see no comment

for this discrepancy. For prediction rejection rate, we confirm the relative performance, and also show that it starts to drop rapidly below their tested range.

4. **Dependency on temperature annealing**: Our results diverge heavily from the results in the paper for temperatures 1 and 2. While the original authors are able to train working but sub-par models with these temperatures, we are unable to get the models to converge at all. We re-did the experiments with a new ensemble, and experimented with the smoothing factor and auxiliary data, but were unable to find any explanation for this difference. Nevertheless, these findings support the claim that temperature annealing is essential for successful use of the EnD^2 method. The authors suggested temperature 5 as a minimum value beyond which larger values make no difference. Our findings support this as well, although our increased resolution reveals that the minimum value for the CIFAR-10 dataset is closer to 3 than 5.

5. **Uncertainty decomposition**: Based on the description in [3] an image with a high knowledge uncertainty should produce a Dirichlet PDF with a close to uniform spread. Our simplex visualizations on the 3-class+AUX dataset shows that this is not the case. This is not too surprising, given that high knowledge uncertainty correlates with small alphas, and this in turn produces convex as opposed to flat probability density surfaces. Overall, these plots suggest that EnD^{2}can capture the uncertainty decomposition of the ensemble.

   The plots also show an interesting behaviour in the ensemble. The ensembles agree to a surprising extent on the out-of-domain samples. In fact, when they do disagree it normally takes the form of data uncertainty as opposed to knowledge uncertainty. This could perhaps shed some light on the observation that knowledge uncertainty does not seem to be useful for OOD-detection on CIFAR-10. The original authors explain this as essentially being a property of the dataset. We feel, based on the visualizations, that another possibility might be that the ensemble models simply are not diverse enough to provide a useful measure of knowledge uncertainty.

5.2 What was difficult

Although the general idea of the paper is well formulated in mathematical terms, the original paper does not provide many hints regarding how to implement the method. In our case, this imposed a significant barrier to immediately reproducing the work, since our inexperience meant that we're unable to immediately see how it could be implemented in a modern deep learning framework. There is some code available in a public repository hosted by one of the authors but this is not mentioned in the paper, and so we could not treat it as an official implementation. We have provided a pseudocode in our supplemental material, in order to hopefully assist future reproducers.
There are also some missing details regarding the models used. Most importantly, the authors mention that they have used a modified VGG model, but do not specify what these modifications are. The authors also do not specify the min and max value of the cyclic LR. These details may explain the consistently worse performance of our models despite the attempt of replication.

5.3 What was easy

The synthetic dataset was fairly easy to reconstruct, and the other datasets are well known and publicly available. The data augmentation was straightforward and easy to incorporate into a training pipeline. The base model (VGG16) used in most of the experiments is well known and was computationally feasible to train. Similarly, the datasets are not excessively demanding in terms of computation, although in our case training

time did become a limiting factor due to the amount of time we spent on implementation and experimentation. The mathematical formulation of the model is very good, helping the conceptual understanding.

5.4 Communication with original authors

We did not communicate with the authors while reproducing their work, although we did refer to some resources which one of the authors has made publicly available, including an repository [3] made for [3] containing an implementation of EnD^2. At the same time as submitting this report, we also sent a copy to the authors and asked for their comments.

References

1. B. Lakshminarayanan, A. Pritzel, and C. Blundell. "Simple and Scalable Predictive Uncertainty Estimation using Deep Ensembles." In: **Advances in Neural Information Processing Systems 30**. 2017.
2. A. Malinin, B. Mlodozeniec, and M. Gales. "Ensemble Distribution Distillation." In: **International Conference on Learning Representations (ICLR)**. 2020.
3. A. Malinin and M. Gales. "Predictive Uncertainty Estimation via Prior Networks." In: **Advances in Neural Information Processing Systems 31**. 2018.
4. G. Hinton, O. Vinyals, and J. Dean. "Distilling the Knowledge in a Neural Network." In: **NIPS Deep Learning and Representation Learning Workshop**. 2015.
5. A. Krizhevsky. "Learning Multiple Layers of Features from Tiny Images." In: **University of Toronto** (May 2012).
6. F. Yu, Y. Zhang, S. Song, A. Seff, and J. Xiao. "LSUN: Construction of a Large-scale Image Dataset using Deep Learning with Humans in the Loop." In: **CoRR** abs/1506.03365 (2015). arXiv:1506.03365. URL: http://arxiv.org/abs/1506.03365.
7. K. Simonyan and A. Zisserman. "Very Deep Convolutional Networks for Large-Scale Image Recognition." In: **International Conference on Learning Representations (ICLR)**. 2014.

[3] https://github.com/KaosEngineer/PriorNetworks/tree/master/prior_networks

A The EnD^2 Algorithm

The original paper features an excellent description of the mathematical formulation of the EnD^2 model, but we did not find it immediately obvious how to translate this into an implementation in a modern deep learning framework. For this reason, we will now briefly describe it from an algorithmic-centred perspective using pseudocode and plain English.

The process of training an EnD^2 model is described in Algorithm 1. In practice, the optimization in line 7 can easily be achieved using the standard "fit" method of frameworks such as Keras and PyTorch, by constructing an intermediate dataset and using a custom loss function with a callback for annealing the temperature.

The intermediate dataset is constructed by first adding any auxiliary images to the training images, and then passing the extended image set as input to the ensemble. The ensemble should output an array of logits as described in line 5 of Algorithm 1. The new dataset is then formed by matching each image to its corresponding ensemble logits, using the latter as the target.

The custom loss function is described in Algorithm 2. This formulation includes temperature annealing. This loss function is the only modification necessary to adapt a general classification model into an EnD^2 model, providing it is then trained on an intermediate dataset as described in the previous paragraph. Note that this formulation assumes that the model outputs logits. This output can be converted into Dirichlet probabilities by applying the standard softmax operation.

Algorithm 1: Training algorithm for EnD^2 given an ensemble

Input : Ensemble En outputting logits, training data X (same as the ensemble is trained on), (optional) Out of distribution data X_{OOD}

Output : Trained EnD^2 model

1 **if** X_{OOD} **not None then**
2 $\quad X = [X, X_{OOD}]$ // append OOD data to training set
3 **end**
4 $\phi = En.predict(X)$ // $\exp(\phi)$ are the labels for EnD^2
5 // ϕ is a tensor of logits corresponding to the true distribution, each row corresponds to a model and each column a class. Each matrix corresponds to one image
6 $model_\theta \leftarrow classifier$ //create a new classifier model with weights θ, with logits as output
7 EnD^2 $= argmin_\theta\{Loss_{EnD^2}(\phi, model_\theta(X))\}$ //train model backpropagation
8 return EnD^2

B Experiments on Synthetic Data

B.1 Methodology

The goal with these experiments is to provide qualitative justification for Claim 5 and illustrate the inner workings of EnD^2. We also provide some new experiments on temperature annealing and the size of the auxiliary dataset, to visualize their effect.

Dataset — To illustrate the model, Malinin et. al. use a synthetic dataset in $\mathbb{R}^2$. Our rendering of this dataset can be seen in Figure 6. This is advantageous since it enables plotting both knowledge and data uncertainty over the entire data manifold, giving a qualitative understanding of whether the algorithm works or not, in contrast to higher

Algorithm 2: loss for EnD^2

Input : Ensemble logits: ϕ, predicted logits: z, temperature: $T = T(t)$, annealing
Output : cost: C

$\epsilon = 10^{-8}$ // Smoothing factor
$\delta = 1 - 10^{-3}$ // Central smoothing factor
$\alpha = e^{z/T(t)}$ // elementwise exponential
M = #models
N = #classes
for $i \leftarrow 1$ **to** M **do**
  $\alpha_{0i} = \sum_j \alpha_{i,j}$ // sum over the classes to produce the precision factor
end
$P_{En} = softmax(\phi/T(t))$ // softmax over classes
$P_{En} = \delta(P_{En} - \frac{1}{N}) + \frac{1}{N}$
$TIT = \sum_i^N (log(\Gamma(\alpha_i + \epsilon))) - log(\Gamma(\alpha_0 + \epsilon))$ // target independent term, where $log(\Gamma(x)) = log((x-1)!)$
$A = \frac{1}{M} \sum_i^M (log(P_{En_i} + \epsilon)$ // mean over ensemble
$TDT = -\sum_i^N ((\alpha_i - 1)A_i)$ // target dependent term, sum over classes
return $(TDT + TIT)T(t)^2$

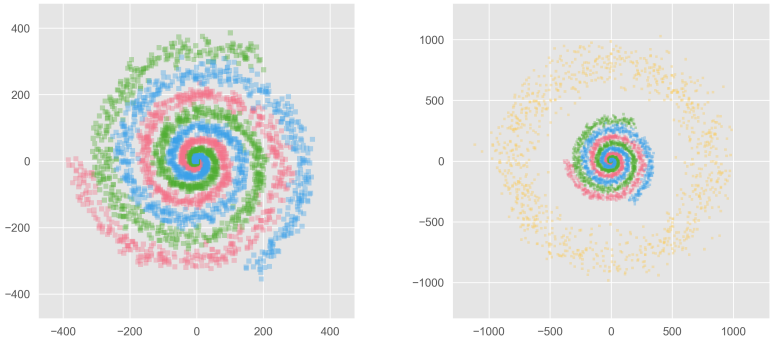

Figure 6. The synthetic, spiral dataset.

dimensional data (images, etc.) that cannot be plotted. The dataset itself looks like a spiral, divided into three classes shaped as spiralling arms of increasing radius. The spirals are centred and almost symmetric around the origin. Furthermore, they have increased noise and overlap with radius, which leads us to believe that uncertainty should vary as well. In addition to the spiral data an OOD data-set, referred to as the AUX data-set is also used, which takes the form of a ring slightly outside the spiral.
For the experiments, 1000 samples per ID class are used, both for training and test. The number of AUX samples was also 1000. This is the same setting as the original paper. The generation of the data uses the original paper's code, but the hyperparameters were not specified. Our hyperparameters can be found in our code. We manually searched for hyperparameters, so that our plot would look as close to theirs, but the exact correspondence is probably not achieved.

Model description and hyperparameters — The original paper does not specify what type of neural network was used for classification. We were also unable to find it in the (unofficial) code. Instead, we chose to use a simple DNN with four hidden layers, each of width

Table 5. Classification error on Spiral Dataset, compared with [2]. Error bars are 95%-confidence intervals assuming normal distribution. Note that our results likely use a different base model and training procedure than the original paper, since it was not specified there.

ERR↓	IND	ENSM	EnD	EnD^2	EnD +AUX	EnD^2 +AUX	EnD^2 +AUX,ANN	EnD^2 +AUX,T=2.5	EnD^2 +AUX20
Our results	8.20±0.67	2.3±NA	3.90±0.65	3.86±0.70	2.61±0.11	4.67±3.26	3.30±0.59	3.45±0.96	5.0±1.54
Paper [2]	13.21	12.37	12.39	12.47	12.41	12.40	-	-	-

64 with ReLu-activation functions, trained by minimizing the categorical cross-entropy using the Adam-optimizer, all with standard `tf.keras` settings, for 85 epochs. EnD and EnD^2 used the same base model but was instead trained for 500 epochs.

Experimental setup and code — On the output of an ensemble of 100 models, all differently randomly initialized, we train EnD and EnD^2 both with and without auxiliary data, using an initial temperature of 1, as in the paper. Doing this, we observed that the training diverges for many initialisations, mainly for $\text{EnD}^2_{\text{+AUX}}$. Thus, we also used an initial temperature of $T = 2.5$, both with and without annealing. The annealing schedule was $T = 2.5$ between epoch 0 and 200, linearly decreasing to 1 between epoch 200 and 400 and 1 between epoch 400 and 500. Additionally, we also trained a model $\text{EnD}^2_{\text{+AUX20}}$, with only 20 samples from the auxiliary dataset.
All 7 models were trained 20 times, with different random initialisations. To make sure they converged, the test error was calculated. In cases test error was above 10%, it was deemed as non-convergence, and not taken into account. Among the converged ones, the mean error and the 95%-confidence interval around the mean is calculated, assuming a normal distribution. This means that for cases with fewer samples, the confidence interval is larger.
The main goal of this experiment is to visually show the total uncertainty, the data uncertainty and the knowledge uncertainty. They were calculated as specified in [2] and [3], for the grid $[-2000, 2000] \times [-2000, 2000]$ at all coordinates divisible by four, for a total of 10^6 points.
The full code is available at https://anonymous.4open.science/r/4ee2c9ef-295f-44e2-8214-f0818b932817/.

Computational requirements — The experiments were run on the CPU of a normal laptop (2.7 GHz Dual-Core i5). The total time to reproduce the ensemble of 100 models and all 20 repetitions of all 7 tested distillation methods, is around 5 to 6 hours.

B.2 Results

Classification accuracy — In Table 5, the classification accuracy from our experiment and the original paper is reported. We see that

- the ensemble outperforms the individual models, and that all distillation methods perform closer to the ensemble, than an individual model.
- the best performance is achieved by EnD with auxiliary data.
- using annealing or not when starting at $T = 2.5$ does not affect the final classification accuracy.

Table 6. Computation requirements for major experiments, and which claims they test. GPU time refers to time on an NVIDIA GeForce RTX 2070. Equivalent cost represents the cost if run on a V100 on Google cloud, for $2.48 per hour.

Experiment	Models	GPU min/model	GPU days	Eqv. cost (USD)
Ensemble, training	400	16	4.44	91.53
Ensemble, labeling	400	0.45	0.13	2.57
Ensemble, inference	400	0.23	0.06	1.32
Evaluation, claim 1 and 2	15	51	0.53	10.94
Size ablation, training, claim 3	112	51	3.97	81.69
Temperature ablation, training, claim 4	27	51	0.96	19.69
3-class ensemble, training, claim 5	100	5.25	0.36	7.51
Total			11.413	235.06

Visualization of uncertainty — The total, data and knowledge uncertainty is plotted in Figure 7 for a grid of 10^6 points. In contrast to the original paper, we fix the scale of the colour bar for better comparability between plots.
We observe that

- EnD^2 is not able to emulate the uncertainty landscape of the ensemble, but EnD$^2_{+\text{AUX}}$ can approximate it fairly well.
- Starting at a higher temperature ($T = 2.5$) and using annealing produces similar results as starting at temperature 1, but starting at temperature 2.5 and keeping it there for the entire training duration does not capture the true uncertainty.
- Using a smaller auxiliary dataset gives a worse approximation of the ensemble's uncertainty landscape.

C Computational requirements for reproduction

In this section, we report the computational resources used for this reproduction. The running time of the major experiments on CIFAR-10 is expressed in time on an RTX 2070. For easier comparison, we also report the equivalent cost when running on a V100 GPU on Google Cloud for $2.48 per hour, given a relative performance of 2.89 versus an RTX 2070[4]. Note that these figures represent the time to reproduce only the final experiments. We estimate that the total GPU time used for this reproduction, including experimentation and bug-hunting, to be 3 to 5 times as long. The full data can be seen in Table 6.

D Histograms

To compare ensembles, EnD^2 and EnD$^2_{+\text{AUX}}$ on the CIFAR-10 and 3-class CIFAR-10 datasets, we provide histograms of data and knowledge uncertainty for in- and out-of-domain-distribution, in Figure 8 and 9.

[4]Benchmark taken from https://timdettmers.com/2020/09/07/which-gpu-for-deep-learning/

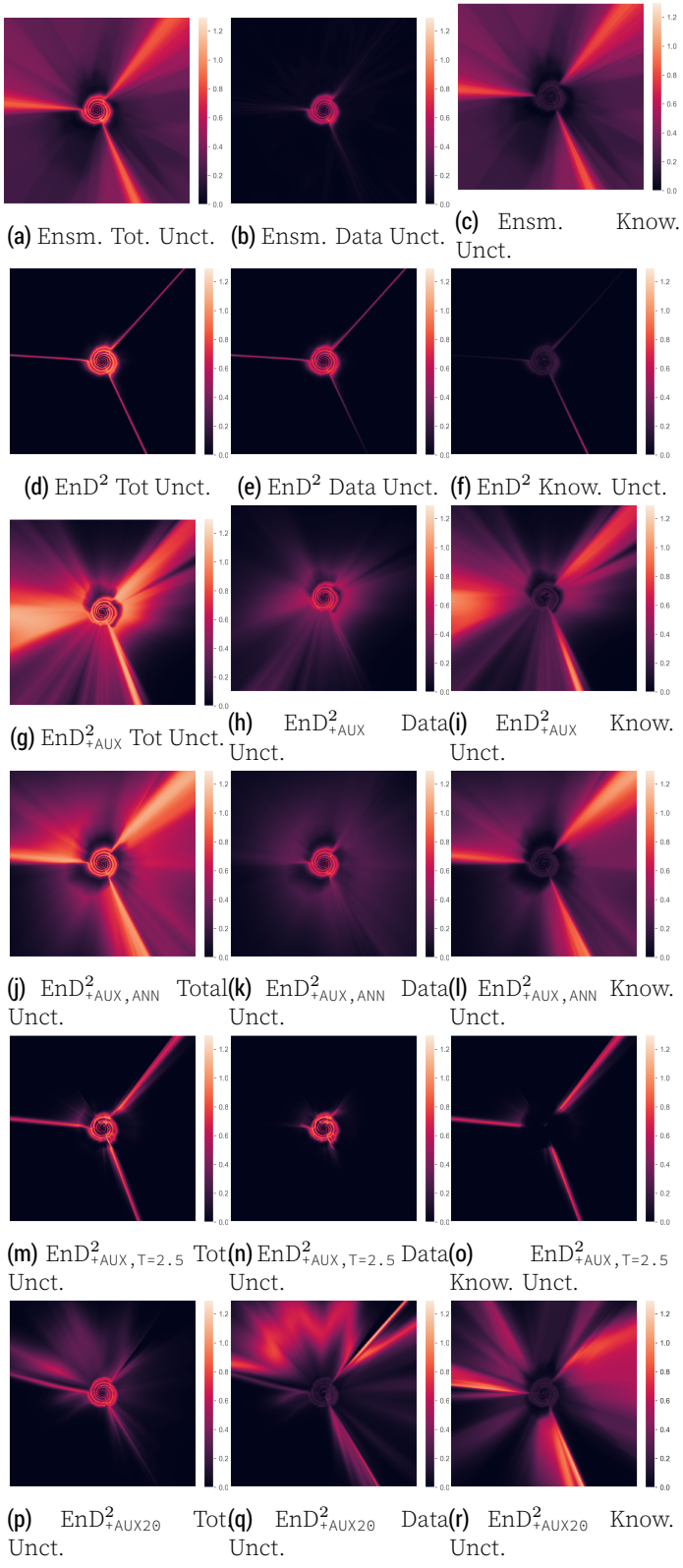

(a) Ensm. Tot. Unct. **(b)** Ensm. Data Unct. **(c)** Ensm. Know. Unct.

(d) EnD^2 Tot Unct. **(e)** EnD^2 Data Unct. **(f)** EnD^2 Know. Unct.

(g) EnD$^2_{+\text{AUX}}$ Tot Unct. **(h)** EnD$^2_{+\text{AUX}}$ Data Unct. **(i)** EnD$^2_{+\text{AUX}}$ Know. Unct.

(j) EnD$^2_{+\text{AUX},\text{ANN}}$ Total Unct. **(k)** EnD$^2_{+\text{AUX},\text{ANN}}$ Data Unct. **(l)** EnD$^2_{+\text{AUX},\text{ANN}}$ Know. Unct.

(m) EnD$^2_{+\text{AUX},\text{T=2.5}}$ Tot Unct. **(n)** EnD$^2_{+\text{AUX},\text{T=2.5}}$ Data Unct. **(o)** EnD$^2_{+\text{AUX},\text{T=2.5}}$ Know. Unct.

(p) EnD$^2_{+\text{AUX20}}$ Tot Unct. **(q)** EnD$^2_{+\text{AUX20}}$ Data Unct. **(r)** EnD$^2_{+\text{AUX20}}$ Know. Unct.

Figure 7. Recreation of Figure 3 in [2], showing uncertainties over entire data manifold.

Table 7. OOD ROC-AUC↑ on CIFAR-10 (in) and LSUN (out), normalized to ensemble results. Error bounds signify two standard deviations, taken over three models.

Unc.	IND	ENSM	EnD	EnD^2	$\text{EnD}_{\text{+AUX}}$	$\text{EnD}^2_{\text{+AUX}}$	PN $_{\text{+AUX}}$
Tot. our	$0.96_{\pm 0.00}$	$1.00_{\pm NA}$	$1.00_{\pm 0.01}$	$0.98_{\pm 0.00}$	$1.01_{\pm 0.00}$	$1.00_{\pm 0.00}$	$\mathbf{1.02}_{\pm 0.01}$
Tot. paper	$0.97_{\pm 0.01}$	$1.00_{\pm NA}$	$0.94_{\pm 0.01}$	$0.97_{\pm 0.01}$	$0.94_{\pm 0.01}$	$1.00_{\pm 0.01}$	$\mathbf{1.01}_{\pm 0.01}$
Know., our	-	$1.00_{\pm NA}$	-	$0.95_{\pm 0.01}$	-	$0.99_{\pm 0.01}$	$\mathbf{1.02}_{\pm 0.00}$
Know., paper	-	$1.00_{\pm NA}$	-	$0.98_{\pm 0.01}$	-	$0.99_{\pm 0.01}$	$\mathbf{1.01}_{\pm 0.01}$

E Relative performance of EnD^2 compared to ensemble and original article

In Tables 3 and 4 of the main report we report several measures for the 7 different models tested. For better comparability, we here also provide the values normalized to the ensembles' performance, both for our experiments, and for the original paper, in Table 8 and 7.

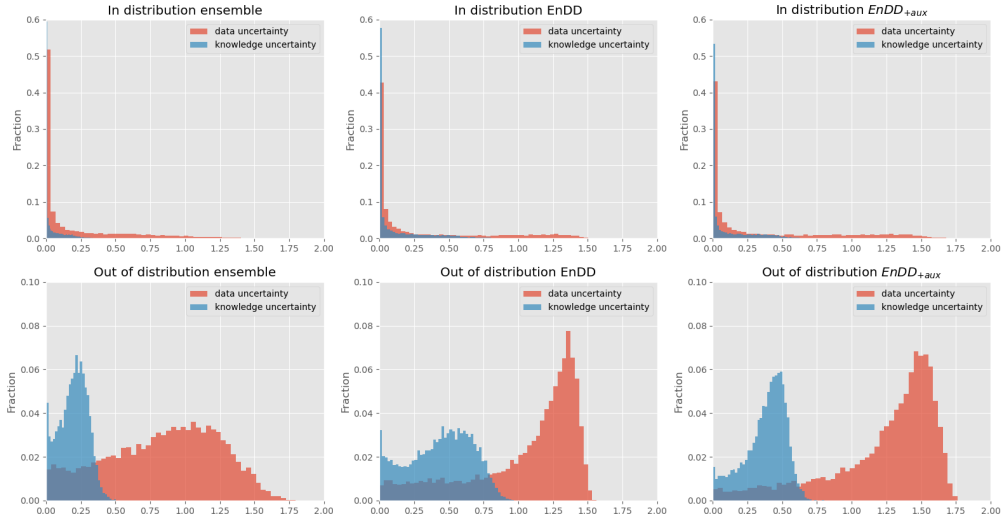

Figure 8. Data/knowledge uncertainty-distributions for ensemble, EnD^2 and $\text{EnD}^2_{\text{+AUX}}$.

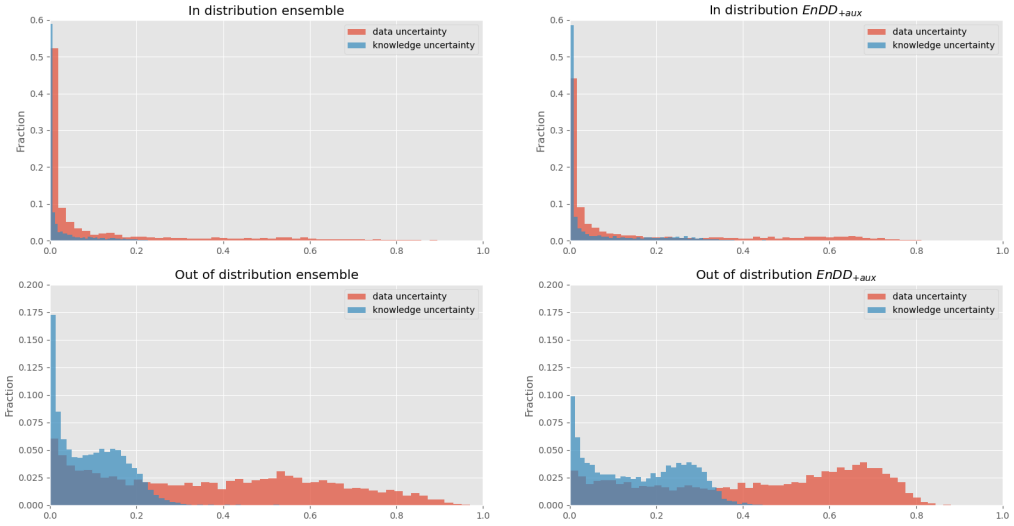

Figure 9. Data/knowledge uncertainty-distributions for ensemble and $\text{EnD}^2_{+\text{AUX}}$ on the 3-class CIFAR10 dataset

Table 8. Classification metrics on CIFAR-10, normalized to ensemble results. Error bounds signify two standard deviations, taken over three models.

Crit.	IND	ENSM	EnD	EnD^2	$\text{EnD}_{+\text{AUX}}$	$\text{EnD}^2_{+\text{AUX}}$	$\text{PN}_{+\text{AUX}}$
ERR↓, our	1.12±0.08	1.00±NA	**0.99**±0.06	1.13±0.02	1.13±0.02	1.16±0.01	1.14±0.04
ERR↓, paper	1.29±0.06	**1.00**±NA	1.08±0.05	1.18±0.03	1.08±0.03	1.11±0.06	1.21±0.10
PRR↑, our	0.87±0.02	**1.00**±NA	0.98±0.00	0.96±0.01	0.98±0.02	0.96±0.01	0.70±0.12
PRR↑, paper	0.97±0.01	**1.00**±NA	0.98±0.01	0.98±0.01	0.98±0.00	0.99±0.00	0.94±0.02
ECE↓, our	41.37±0.35	1.00±NA	**0.94**±0.05	1.45±0.13	1.08±0.19	1.85±0.29	5.69±0.37
ECE↓, paper	1.69±0.31	1.00±NA	2.00±0.15	**0.77**±0.15	2.00±0.46	1.69±0.31	9.23±0.54
NLL↓, our	6.38±0.04	**1.00**±NA	1.06±0.04	1.35±0.02	1.19±0.01	1.38±0.01	1.86±0.04
NLL↓, paper	1.32±0.05	**1.00**±NA	1.16±0.05	1.32±0.05	1.16±0.05	1.26±0.00	2.00±0.05